Sensitivity of middle atmospheric temperature and circulation in the UIUC GCM to the treatment of subgrid-scale gravity-wave breaking

Working Paper

Author(s):
Yang, F.; Schlesinger, Michael E.; Rozanov, Eugene; Andronova, Natalia; Zubov, V.A.; Callis, L.B.

Publication date:
2006-09-25

Permanent link:
https://doi.org/10.3929/ethz-b-000023910

Originally published in:
Atmospheric Chemistry and Physics Discussions 6(5), https://doi.org/10.5194/acpd-6-9085-2006

Atmos. Chem. Phys. Discuss., 6, 9085–9121, 2006
www.atmos-chem-phys-discuss.net/6/9085/2006/

Atmospheric Chemistry and Physics Discussions

Sensitivity of middle atmospheric temperature and circulation in the UIUC GCM to the treatment of subgrid-scale gravity-wave breaking

F. Yang[1,*], M. E. Schlesinger[1], E. V. Rozanov[2], N. Andronova[1], V. A. Zubov[3], and L. B. Callis[4]

[1]Department of Atmospheric Sciences, University of Illinois at Urbana-Champaign, Urbana, Illinois, USA
[2]PMOD/WRC and IAC ETHZ, Davos, Switzerland
[3]A. I. Voeikov Main Geophysical Observatory, St. Petersburg, Russia
[4]Consultant, Suffolk, Virginia, USA
[*]now at: NCEP/EMC, Camp Springs, Maryland, USA

Received: 14 July 2006 – Accepted: 6 September 2006 – Published: 25 September 2006

Correspondence to: F. Yang (fanglin.yang@noaa.gov)

Abstract

The sensitivity of the middle atmospheric temperature and circulation to the treatment of mean-flow forcing due to breaking gravity waves at the sub-grid scale was investigated using the University of Illinois at Urbana-Champaign 40-layer General Circulation Model (GCM). The gravity-wave forcing was represented either by Rayleigh friction or by a detailed parameterization scheme with different sets of parameters. The modeled middle atmospheric temperature and circulation exhibit large sensitivity to the parameterized sub-grid gravity-wave forcing. A large warm bias of up to 50°C was found in the model's summer upper mesosphere and lower thermosphere. This warm bias was caused by the inability of the GCM to simulate the reversal of the zonal winds from easterly to westerly crossing the mesopause in the summer hemisphere. Attempts were made to slow down the easterly winds near the mesopause and to reduce the warm bias. The GCM was able to realistically simulate the semi-annual oscillation in the upper stratosphere and lower mesosphere with observational constraints on certain parameter values, but failed to simulate the quasi–biennial oscillation in any of the experiments. Budget analysis indicates that in the middle atmosphere the forces that act to maintain a steady zonal-mean zonal wind are primarily those associated with the meridional transport circulation and breaking gravity waves. Contributions from the interaction of the model-resolved eddies with the mean flow are secondary.

1 Introduction

It has long been recognized that atmospheric gravity waves have strong effects on atmospheric temperature and circulation. They transport energy and momentum, produce turbulence and mixing, and modify the mean circulation and thermal structure of the atmosphere (for a review see Fritts and Alexander (2003), and references therein). In the past two decades a number of schemes (e.g., Palmer et al., 1986; McFarlane, 1987; Fritts and Lu, 1993; Lott and Miller, 1997) have emerged that parameterize the

ACPD

6, 9085–9121, 2006

drag effect of topographic gravity waves on the mean flow in GCMs. Almost all current atmospheric GCMs have adopted some scheme to treat topographic gravity-wave forcing in the troposphere and lower stratosphere, and for some cases through the entire atmosphere. GCMs including these schemes are able to simulate much better the tropospheric jets, sea-level pressure and surface winds in the northern middle to high latitudes (Hamilton, 1997). However, the progress in developing parameterization schemes for either stationary or non-stationary gravity waves suitable for use in the middle atmosphere has been relatively slow due to limitations in both theoretical understanding and field observations. Accordingly, Rayleigh friction was chosen by many GCM modelers to crudely treat the forcing effects of breaking gravity waves in the middle atmosphere (e.g., Beagley et al., 1996; Manzini and Bengtsson, 1996; Langematz and Pawson, 1997; Swinbank et al., 1998). In recent years, however, considerable advances have been made in the observation, theoretical understanding and modeling of middle atmospheric gravity waves. The advances have led to a number of parameterizations that are applicable for GCMs to describe the forcing by gravity-wave breaking on the large-scale circulation in the middle atmosphere (e.g., Medvedev and Klaasen, 1995; Hines, 1997a, b; Alexander and Dunkerton, 1999; Warner and McIntyre, 2001). Many of these schemes are now in different stages of testing and implementation by GCM groups.

At the University of Illinois at Urbana-Champaign (UIUC) a 40-layer mesosphere-stratosphere-troposphere general circulation model (MST-GCM) was developed based on the UIUC 24-layer stratosphere-troposphere (ST) GCM (Yang et al., 2000). This 40-layer GCM extends up to the lower thermosphere with its top at 0.00084 hPa (about 98 km; Fig. 1). One application of the GCM is to study the impact of solar variability on atmospheric chemical composition and climate. Special attention has been paid to the simulation of upper atmospheric temperature and circulation because they influence atmospheric chemical reactions and the transport of atmospheric constituents. To parameterize the forcing of breaking gravity waves on the mean flow in the middle atmosphere, the scheme of Rayleigh friction, which was introduced by Holton and

ACPD
6, 9085–9121, 2006

EGU

Wehrbein (1980) and used in the UIUC 24-layer GCM, was first expanded and tested. Unsatisfied with the outcome, we have adopted the more physically based scheme of gravity-wave breaking parameterization developed by Alexander and Dunkerton (1999) (hereinafter referred to as AD).

Like other current schemes, the AD scheme contains a set of tuning parameters that defines the source of gravity waves and the distribution of momentum forcing due to gravity-wave breaking. The AD-1999 paper established its theoretical foundation of the scheme; however, the tuning parameters were allowed to vary considerably to accommodate different situations and were only loosely constrained by limited observations. By making use of satellite observations and the UK Met Office-analyzed wind and temperature fields, Alexander and Rosenlof (2003) (hereinafter referred to as AR-2003) derived estimates of gravity-wave mean flow forcing, and then inferred constraints on gravity waves that germinate near the tropopause and dissipate in the stratosphere.

In the present study we document four experiments, one utilizing Rayleigh fiction and the others utilizing the AD scheme with three different sets of parameters, to test the sensitivity of the middle atmospheric temperature and circulation to the forcing of breaking gravity waves in the UIUC MST-GCM. For the AD scheme, the first two sets of the parameters were chosen based on the recommendations given in the AD-1999 paper and the AR-2003 paper, respectively. No attempts of tuning were made. The third set of parameters documented here were based on the AR-2003 paper and resulted from extensive tuning and experimentation that were aimed to obtain a better performance of the GCM as a whole and, in particular, the simulation of temperature and circulation in the mesosphere. Given the excessively broad range of tuning parameters in current gravity-wave drag parameterizations and inadequate constraints from observations, lessons learned here may shed some light on future development of gravity-wave forcing parameterization for GCMs.

The paper is organized in the following way. Section 2 describes briefly the structure of the UIUC 40-layer MST-GCM and its major difference from the UIUC 24-layer ST-GCM. The updates on the terrestrial and solar radiation modules that accommo-

ACPD
6, 9085–9121, 2006

EGU

date special needs for middle atmospheric modeling, and the corresponding changes in atmospheric heating rates, are elaborated in some detail. Section 3 describes the tests of Rayleigh friction, and three sensitivity experiments with the AD scheme. Offline tests were carried out with standard atmospheric profiles to compare their forcing characteristics. Section 4 compares the simulated middle atmospheric temperature and circulation with observations. The maintenance of the zonal-mean zonal winds in the middle atmosphere is examined. Section 5 presents our conclusions.

2 Model description and updates on the radiative transfer modules

The 40-layer MST-GCM was developed based on the UIUC 24-layer ST GCM (Yang et al., 2000). The 24-layer ST-GCM has been used for many studies, such as the reconstruction of the radiative forcing of historical volcanic eruptions (Andronova et al., 1999), simulations of climatic changes induced by the Pinatubo volcanic eruption (Yang and Schlesinger, 2002; Rozanov et al., 2002) and participation in the Second Atmospheric Model Intercomparison Project (Gleckler, 1999). It has also been coupled with the UIUC atmospheric chemical transport model (ACTM) to simulate the distributions of source gases and ozone in the stratosphere (Rozanov et al., 1999a,b), and the climatic changes caused by the increase of solar UV radiation from solar minimum to solar maximum (Rozanov et al., 2004). The primary applications of the 40-layer GCM are to study the response of the atmosphere to energetic electron precipitation (Rozanov et al., 2005) and the impact of solar variability on atmospheric chemical composition and climate. Major efforts have been made to simulate better the temperature and circulation of the middle atmosphere because of their great impact on middle atmospheric chemical reactions and transport.

The 40-layer MST-GCM has a horizontal resolution of 4° latitude by 5° longitude. Vertically the model extends from the earth's surface to 0.00084 hPa (about 98 km; Fig. 1). The model uses sigma (σ) as its vertical coordinate, such that the earth's surface is the coordinate surface σ=1 and the top of the model is the coordinate surface

ACPD
6, 9085–9121, 2006

EGU

σ=0. The layers in the troposphere were prescribed and chosen to best resolve the boundary layer and the tropopause. Above the tropopause (~120 hPa to model top), the thickness of the layers gradually increases and follows the prescription,

$$\ln\left(\frac{P_k}{P_{k+1}}\right) \Big/ \ln\left(\frac{P_{k+1}}{P_{k+2}}\right) = 1.05, \quad (1)$$

where P_k is the pressure for the integer level k within the layer, with k increasing downward.

The 40-layer MST-GCM shares the same dynamical and physical packages as the 24-layer ST-GCM except the changes described here. The parameterization for long-wave (LW) radiative transfer of the 24-layer ST-GCM was developed by Chou and Suarez (1994) and modified by Yang et al. (2000). It did not resolve non-local thermodynamical equilibrium (non-LTE) in the upper atmosphere. Therefore, the formulation of Fomichev et al. (1998) was adopted to replace the Chou and Suarez (1994) module in the upper atmosphere above 0.02 hPa to calculate LW heating. Non-LTE condition for the 15 μm CO_2 band was accounted for. Additional absorption of solar radiation in the model atmosphere above 0.1 hPa by O_2 at the Lyman-alpha line, Schumann-Runge band and Herzberg continuum was also parameterized using the Strobel (1978) formalism.

To treat the mean-flow forcing due to breaking subgrid-scale gravity waves, the parameterization of Palmer et al. (1986) was included to describe topographic gravity-wave forcing in the troposphere and middle to lower stratosphere below 10 hPa. For nin-topographic gravity-wave forcing, either Rayleigh friction or the AD parameterization was used depending upon the experimental type of this study. In addition, a momentum damping (Hansen et al., 1983) was applied to both the zonal and meridional winds in the top two layers of the model. This damping acts to absorb vertically propagating waves forced from below, keeps the model from suffering computational instability, and allows larger time-integration steps to be used.

To estimate the changes in heating rates due to the introduction of the 15 μm CO_2 band non-LTE condition, LW heating rates were compared between the Chou and

Suarez (1994) and Fomichev et al. (1998) schemes in a column model for five standard atmosphere profiles (mid-latitude summer, mid-latitude winter, sub-arctic summer, sub-arctic winter and tropics; (McClatchey et al., 1972)) under clear-sky condition without aerosols. Figure 2 shows the resultant heating rates between 10 and 0.003 hPa for the five cases. Large discrepancies between the two schemes are found in the upper mesosphere and lower thermosphere where both non-LTE and LTE are important. The Chou-Suarez parameterization largely overestimated the magnitude of the LW heating rates in summer near the model top. Based on these tests, for the layers of the MST-GCM above 0.02 hPa, the LW heating rates derived from the Fomichev et al. (1998) scheme were used to replace those from the Chou-Suarez scheme. (It should be pointed out that the two schemes include different gas species. The Chou-Suarez scheme includes H_2O, CO_2, O_3, N_2O, CH_4, CFC11, CFC12, and CFC22. The Fomichev scheme includes CO_2, O_3, O_2, N_2, and O. However, the dominant contributors to LW heating in the upper mesosphere and lower thermosphere are CO_2 and O_3).

Solar radiative transfer in the 40-layer MST-GCM was developed by Chou and Suarez (1999) and modified by Yang et al. (2000) to treat the scattering and absorption by aerosols. Absorption of solar radiation by oxygen is the primary heating source in the upper mesosphere. Chou and Suarez (1999) treats only the O_2 A and B bands (12 850–13 190 and 14 310–14 590 1/cm), and hence underestimated the solar heating by O_2 in the upper atmosphere. We added a subroutine to compute the solar absorption by O_2 based on Strobel (1978) with modifications. It computes O_2 absorption for the Lyman-alpha line and the Schumann-Runge band and Herzberg continuum for layers above 0.1 hPa. This addition increased the solar heating rate by about 2°C/day near the mesopause for a mid-latitude summer atmosphere.

ACPD
6, 9085–9121, 2006

EGU

3 Case definition and off-line calculation using standard atmospheric profiles

In this study we compare four cases of mean-flow forcing due to gravity-wave breaking, one based on Rayleigh friction, and the others from the Alexander and Dunkerton (1999) parameterization. These cases are defined below.

In previous studies, different types of Rayleigh friction have been used in middle atmospheric GCMs (e.g., Swinbank et al., 1998), but they all act to damp the zonal winds with vertically varying relaxation time scales. We adopted the hyperbolic-tangent form introduced by Holton and Wehrbein (1980), with slight modifications gained from tuning experience that enable the 40-layer MST-GCM to simulate better the middle atmosphere circulations. The friction coefficient was determined by

$$\gamma = -\frac{1}{\alpha}\left[1 + \tanh\left(\frac{z - z_0}{d}\right)\right] \quad , \text{days}^{-1}, \tag{2}$$

where z is the height of a layer in km, z_0 equals 54 km in the Northern Hemisphere and 56 km in the Southern Hemisphere, and d=7.5 km. For westerly winds, α=3; for easterly winds, α=15 in the Northern Hemisphere and α=30 in the Southern Hemisphere. The coefficient γ gradually increases with height. In the 40-layer MST-GCM, Rayleigh friction was applied only for layers above 10 hPa.

Alexander and Dunkerton (1999) developed a parameterization based on the convective instability criterion of Lindzen (1981), and assumed the momentum fluxes carried by gravity waves are all deposited locally at the level of linear wave breaking (Lindzen and Holton, 1968). In principle the parameterization can be used to describe mean-flow forcing due to either stationary gravity waves excited by mountains or non-stationary gravity waves from sources like convection and wind shear, or both. In any circumstance, the input of gravity-wave momentum flux is usually specified at a level in the upper troposphere to the lower stratosphere. Even though there have been some estimates, the strength of this input for either stationary or non-stationary sources is still poorly constrained, primarily because of insufficient observations (Fritts and Alexander, 2003). To avoid the complication of tuning the parameters related to

ACPD
6, 9085–9121, 2006

EGU

both sources, which are all rather uncertain, we chose to keep the parameterization of Palmer et al. (1986) in the 40-layer MST-GCM to account for the mean-flow forcing due to topographic gravity waves in the troposphere and lower stratosphere below 10 hPa. The parameterization of Palmer et al. (1986) is now widely used in many climate and weather forecast models. Its use in the UIUC 24-layer ST-GCM greatly improved the model's performance (Yang et al., 2000). By doing so, we concentrate on the parameters that control the breaking and momentum deposition of non-stationary gravity waves.

For the AD scheme, there are a number of tuning parameters that control the source of the gravity waves and the distribution of momentum forcing (see Table 1). In the AD 1999 paper, these parameters were allowed to vary considerably to accommodate different situations and were only loosely constrained by limited observations, although recommendations were given on how to prescribe some of the parameters applicable uniformly over the globe. Current parameterizations of middle atmosphere gravity-wave effects all suffer acutely from the lack of constraints on wave sources and tunable parameters (Fritts and Alexander, 2003). Major efforts are required to better understand gravity-wave characteristics and quantify these parameters. One such effort was performed by Alexander and Rosenlof (2003). They used Upper Atmosphere Research Satellite data and the United Kingdom Meteorological Office analyses of wind and temperature to estimate the mean-flow forcing of gravity waves in the stratosphere, then compared the forcing with that calculated by the AD scheme to infer the constraints on the gravity-wave characteristics near the tropopause. They found that these waves in the tropics substantially differ from those in the extratropics. The latter also varies with season.

We conducted a series of GCM experiments using the AD scheme with different sets of parameters. The purpose is to test the sensitivity of the middle atmospheric temperature and circulation to the forcing of breaking gravity waves in the UIUC MST-GCM, and to improve the model's performance. The selection of the parameters is summarized in Table 1.

ACPD
6, 9085–9121, 2006

EGU

The parameters for experiment AD1999 were prescribed as the default values. They were set globally uniform and did not vary with season. The source of gravity-wave momentum flux was placed at the 10th layer of the model (at about 400 hPa in the tropics). The parameters for experiment AR2003 were set to the values in Table 2 (Overall Tropics case) of the AR 2003 paper for the tropics (15° S, 15° N), and in Table 3 (Seasonal Variation Best Fit case) for all latitudes outside of the tropics. The source of gravity-wave momentum flux was placed near the tropopause, the 16th layer of the model. In the tropics, the parameters depend on the phase of the zonal wind at the source level. Outside the tropics, the constraints on gravity waves were treated differently for the Northern and Southern Hemispheres and for different seasons.

As will be seen in the next section, the two experiments described above failed to simulate the observed summer-hemisphere cold mesopause. In the absence of observational constraints on gravity waves dissipating in the upper atmosphere, we carried out extensive tuning in an attempt to reduce the model bias in the upper atmosphere and to improve the model's performance as a whole. We document here one experiment from the tuning exercise, listed in Table 1 as AR2003_M.

To gain a flavor of the differences among the experiments, we compare off-line gravity-wave forcing for the four cases using the CIRA International Reference Atmosphere (CIRA-86) (Fleming et al., 1988, 1990). The dataset contains monthly mean zonal-mean temperature, zonal wind and geopotential height in 5° intervals covering latitudes from 80° S to 80° N, and in 0.25 log-pressure intervals extending from 1013.0 hPa to 0.0000254 hPa (~120 km). The tests performed here used CIRA data up to 0.00084 hPa (the top layer of the 40-layer MST-GCM). Figure 3 shows, as an example, the accelerations of the zonal-mean flow by the parameterized forcing of gravity-wave breaking in January.

For Rayleigh friction, the forcing always acts to damp the mean flow, is proportional to the strength of the mean flow at a given altitude, and exists at all times and in all places where the scheme is applied. In general, large forcing is found adjacent to the cores of middle atmosphere jets. The largest forcing reaches –25 m/s/day for westerly

ACPD
6, 9085–9121, 2006

EGU

winds and 5 m/s/day for easterly winds in the middle mesosphere. For the AD scheme, unlike Rayleigh friction, the forcing tends to accelerate the mean flow in the middle to lower stratosphere and to decelerate the mean flow in the upper mesosphere, and is not ubiquitous since gravity waves break only under certain circumstances. For the AD1999 and AR2003 cases, the largest forcing is found in the middle to upper mesosphere adjacent to the middle atmosphere jet cores, with a magnitude that reaches 25 to 50 m/s/day for easterly winds and about 10 m/s/day for westerly winds. However, forcings from the two cases drastically differ in the tropics and in the winter upper mesosphere and lower thermosphere. The forcing in the tropics for AD1999 is much stronger than for AR2003. All momentum deposition for AD1999 occurs below the mesopause in both hemispheres. The deposition for AR2003 in the winter hemisphere extends to the model top. For the AR2003_M case, the breaking of waves occurs at a higher altitude with much stronger momentum deposition. The forcing is greater than 100 m/s/day for easterly winds and up to 50 m/s/day for westerly winds in the upper mesosphere and lower thermosphere. This large forcing is found to be necessary, as explained in the next section, for the MST-GCM to simulate the wind reversal near the summer-hemisphere mesopause.

4 MST-GCM simulation results

Four experiments were carried out with the UIUC 40-layer MST-GCM for the cases described in Sect. 3 to test the sensitivity of the middle atmospheric temperature and circulation to the mean-flow forcing by gravity-wave breaking. Each experiment was run for ten years starting from the same initial condition. For lower boundary conditions, sea-surface temperature and sea ice were prescribed to be the AMIP–II (Atmospheric Modeling Intercomparison Project) monthly means, which are the averages from 1979 through 1996 (Gleckler, 1999), and were updated daily by interpolation between consecutive monthly values. The initial condition was derived from the 1979–95 climatology of the NCEP/NCAR reanalysis (Kalnay et al., 1996) for the model atmosphere

ACPD
6, 9085–9121, 2006

EGU

from the earth's surface to 10 hPa, and from the COSPAR International Reference Atmosphere (CIRA-86) (Fleming et al., 1988, 1990) for the model atmosphere above. Data from the UIUC 24-layer ST-GCM restart file were used for variables that are not available from observations. Results from the last 8 years of simulation were analyzed. For a concise presentation, only figures for January are shown and discussed if not otherwise indicated. Similar conclusion can be drawn from the investigation for July.

For model validation, we also used temperature and zonal wind from the CIRA-86 observation for atmosphere above 10 hPa, and from the NCEP/NCAR reanalysis below 10 hPa. We compared the CIRA-86 winds with the more recent URAP wind data from the SPARC and UARS Reference Climatology Projects (Swinbank and Ortland, 2003; Randel et al., 2004) (http://hyperion.gsfc.nasa.gov/Analysis/UARS/urap/home.html). The difference between the two datasets is small in comparison with the bias of the GCM. The use of CIRA-86 or URAP winds for model validation does not change the conclusion.

4.1 Zonal mean zonal wind

Latitude-height cross-sections of the simulated monthly mean zonal–mean zonal winds for January are presented in Fig. 4, together with the corresponding observations. In the troposphere and lower stratosphere, the simulated zonal winds are quite similar to each other for all the cases because the Palmer et al. (1986) topographic gravity-wave drag parameterization was applied for all cases. The strength and location of the observed tropospheric jets are well captured. Compared to the UIUC 24-layer ST-GCM (Yang et al., 2000), this 40-layer GCM greatly improved the simulation of the polar-night jet in the northern lower to middle stratosphere. In the 24-layer GCM, the simulated wintertime polar-night jet was too weak and was shifted equatorward of its observed position. This improvement is attributed mostly to the much higher model top of the 40-layer GCM (Yang, 2000). However, the simulated winds in the middle and upper atmosphere differ considerably from case to case.

For the cases of Rayleigh Friction (Fig. 4b) and AD1999 (Fig. 4c), the GCM failed to

ACPD
6, 9085–9121, 2006

EGU

simulate the observed strong westerly winds in the middle atmosphere. In the observations (Fig. 4a), the westerly jet in the Northern Hemisphere extends from the high-latitude middle stratosphere to the subtropical upper mesosphere, forming an axis of a strong jet that tilts towards the equator. The strongest westerly wind reaches 60 m/s near 30° N at about 0.1 hPa. In the simulations, the jets tend to tilt towards the North Pole. Winds in the mesosphere are too weak. The strongest westerly wind is found near the mid-latitude stratopause. In the Southern Hemisphere, the model was able to capture the observed variation of easterly winds with height; that is, the easterly jets tilt toward the South Pole from the subtropical middle stratosphere to the high-latitude upper mesosphere. Still, for the case of AD1999 the easterly winds are too weak, and for the case of Rayleigh Friction the jets are slightly shifted towards the equator. As described in Sect. 3, the coefficients in Eq. (2) that control the strength of Rayleigh friction have been set differently for easterly and westerly winds, and differently for the Northern and Southern Hemispheres based on tuning exercises. Results from experiments with globally uniform coefficients (not shown) were inferior to Fig. 4b. Other mesospheric GCMs that utilized Rayleigh friction to parameterize gravity-wave forcing also had difficulties in simulating the mesospheric jets.

The AD1999 experiment used globally uniform parameters (Table 1) for all seasons that were not well constrained by observations. The investigation by Alexander and Rosenlof (2003) suggests that, at least for gravity waves that dissipate in the stratosphere, the parameters need to be set differently for the tropics and extratropics, and also differently for different seasons. Indeed, the simulation of the zonal-mean zonal wind is improved for the experiment AR2003 (Fig. 4d). Both the easterly and westerly jets in the stratosphere and mesosphere from AR2003 compare more favorably with observations than those from AD1999. The simulated easterly winds in the southern middle atmosphere look rather realistic. For westerly winds, the jets from the middle stratosphere to upper mesosphere in Fig. 4d now tend to tilt towards the equator, although the strength and location of the jet core are still far from perfect in comparison with the observations. The polar-night jet in the northern stratosphere is too strong.

ACPD
6, 9085–9121, 2006

EGU

For the three experiments described so far, the simulated easterly winds in the upper mesosphere and lower thermosphere are all too strong. The GCM failed to capture the observed transition from easterly wind to westerly wind near the model top in the Southern Hemisphere. The simulated summer mesopause is also too warm (see the next section). We performed an extensive tuning exercise in an attempt to reduce this bias, and also to improve the model simulation as a whole. Because there are no adequate observational constraints on the gravity waves that dissipate in the mesosphere and above, the tuning was guided by comparing the simulated results with observations. We show in Figs. 4e the simulated zonal-mean zonal wind from one of the tuning experiments, AR2003_M, which used parameters similar to those in AR2003. By comparing 3c with 3d one can see that we purposefully increased the forcing on the mean flow (easterly winds) in the southern upper mesosphere and lower thermosphere. By doing so, we were able to slow down the easterly jet in this region (see Figs. 4e). For the case of AR2003_M, compared to the case of AR2003, the input momentum flux outside the tropics at the source level was increased by 50% in both hemispheres (see Table 1). There are also changes in the width of the broad spectrum and the peak momentum flux at zero ground phase speed. The slowdown in Fig. 4e is significant in comparison with Fig. 4d but still not enough to produce the observed transition from easterly to westerly winds near the model top. With Rayleigh friction we were not able to capture this reversal no matter how the parameters were tuned, since Rayleigh friction acts only to damp the mean flow (Shepherd et al., 1996). It still presents a big challenge for many middle atmospheric GCMs to simulate this wind reversal (e.g., Medvedev et al., 1998).

For the AD1999 case, the source of gravity waves was placed at about 400 hPa. As a result, the summertime gravity-wave forcing in the upper mesosphere is too small due to excessive filtering by the lower atmosphere (Fig. 3b). This occurs because the summertime zonal wind reverses from westerly in the troposphere through a zero wind line to strong easterly in the upper stratosphere and mesosphere. Most of the waves encounter critical-level filtering in the troposphere and lower stratosphere. Only

ACPD
6, 9085–9121, 2006

EGU

a small portion of the gravity waves can reach the upper stratosphere and mesosphere. In experiments AR2003 and AR2003_M, the source of gravity waves was placed at a much higher altitude. This allows the model to generate adequate gravity-wave drag to slowdown the easterly near the mesopause.

4.2 Zonal-mean temperature

Figure 5 presents the observed zonal–mean temperature in January and the differences between the model simulations and observation. For all cases the model performed generally well in the troposphere and stratosphere everywhere except in the polar stratosphere. Temperature biases are less than a few degrees in the troposphere and about 10°C in the stratosphere in middle to low latitudes. Near the South Pole, the simulated temperatures are about 20°C colder than the observed in the lower stratosphere.

In the mesosphere and lower thermosphere, for the cases of Rayleigh friction, AD1999 and AR2003 the model failed to simulate the cold polar mesopause in the summer (southern) hemisphere. Near the model's top, large warm biases of more than 50°C are found in the southern high latitudes in January. For the case of AR2003_M, the warm bias is reduced to about 20°C. This observed cold mesopause in the summer hemisphere is closely linked to the reversal of zonal winds from easterly below the mesopause to westerly winds above. It has been known for a long time that, in the mesosphere and lower thermosphere, the mean-flow forcing due to gravity-wave breaking causes the reversal of zonal-mean winds, drives a mean-meridional transport circulation, and leads to a warm winter mesopause and a cold summer mesopause (see the review by Holton and Alexander, 2000, and references therein). In the next section we compare how the transport circulations differ between the four experiments, and how the mean flow is maintained in the atmosphere.

ACPD
6, 9085–9121, 2006

EGU

4.3 Residual circulation and maintenance of the zonal-mean zonal winds in the middle atmosphere

To compare the mean–meridional circulations between the five experiments from a Lagrangian point of view, we computed the residual meridional and vertical winds from the framework of the transformed Eulerian-mean circulation (Andrews and McIntyre, 1976). Formally, the residual circulation is the part of the mean-meridional circulation that is not balanced by the convergence of model-resolved eddy enthalpy fluxes. The calculation was performed using the eddy fluxes of momentum and potential temperature sampled at 6–h intervals and the monthly means of other quantities on isobaric surfaces. For each case, the monthly mean residual circulation for individual years was computed before the multi-year averages were derived.

Figures 6 and 7 present the 8-year-averaged residual meridional wind $[\bar{v}]_r$ and residual vertical wind $[\bar{w}]_r$ from 10 to 0.0014 hPa for the four cases in January. In computing, the approximation $[\bar{\omega}]_r = -[\bar{\rho}]\, g\, [\bar{w}]_r$ was assumed to convert $[\bar{\omega}]_r$ in Pascal/s in p–coordinate to $[\bar{w}]_r$ in cm/s in z–coordinate, where $[\bar{\rho}]$ is the monthly mean zonal–mean air density. For all cases, $[\bar{v}]_r$ is positive in Fig. 6 in the middle mesosphere, indicating a pole-to-pole northward transport in January. Air ascends in the summer mesosphere ($[\bar{w}]_r > 0$) and descends in the winter mesosphere ($[\bar{w}]_r < 0$) (Fig. 7). The residual circulations for the cases of Rayleigh Friction, AD1999 and AR2003 are much weaker than that for the case of AR2003_M, in which $[\bar{v}]_r$ reaches about 4 m/s near the mesopause in the southern middle and high latitudes (Fig. 6d) and the ascending branch of $[\bar{w}]_r$ reaches about 2 cm/s in the middle and upper mesosphere near the South Pole (Fig. 7d). This strong ascending motion leads to a stronger adiabatic cooling; therefore, the warm bias is reduced. Some global and mechanistic model studies suggest that to account for the summer mesopause thermal structure $[\bar{v}]_r$ and $[\bar{w}]_r$ need to reach ~20–30 m/s and 5 cm/s, respectively (for a review see Fritts and Alexander, 2003).

To understand why strong forcing of gravity-wave breaking is required to sustain the

ACPD
6, 9085–9121, 2006

EGU

thermal structure in the middle atmosphere, we consider further how the zonal-mean flow is maintained in the atmosphere, as an example, for the case of AR2003_M. In the spherical pressure coordinate system and in the framework of transformed Eulerian mean circulation, the tendency of the zonal-mean zonal wind can be written as (Peixóto and Oort, 1992),

$$\frac{\partial [u]}{\partial t} = f\,[\bar{v}]_r + \frac{1}{R\cos\phi}\mathrm{div}\boldsymbol{F} + [F_\lambda]\,, \tag{3}$$

where div$\boldsymbol{F}$ is the divergence of the Eliassen-Palm (EP) flux, $[F_\lambda]$ represents the frictional force near the earth's surface, and, for GCMs, any parameterized forces that are not explicitly resolved by the model's dynamical processes, including those due to gravity-wave breaking, sponge-layer friction, diffusion and convection. The strength of the EP flux measures the interaction between the mean flow and eddy disturbances, and the divergence of EP flux reflects the momentum forcing due to model-resolved eddies that interact with the mean flow. For a long-term mean, $\partial [u]/\partial t \rightarrow 0$, hence the three terms on the right-hand side of Eq. (3) should be in balance.

Figures 8a and b depict the derived 8-year mean EP-flux divergence ($div\boldsymbol{F}/R\cos\phi$) and the forcing on the mean flow due to the meridional residual winds ($f\,[\bar{v}]_r$) in January for the case of AR2003_M. To obtain $[F_\lambda]$, we accumulated the changes in the zonal-mean zonal wind due to the different forcings that are not explicitly resolved by the GCM but are instead parameterized, at each time step during model integration and saved the output of monthly means. Shown in Figs. 8c and d are the zonal-mean tendencies of the zonal wind in January contributed by the breaking of non-topographic gravity waves (the AD parameterization, Fig. 8c), and by the breaking of topographic gravity waves (Palmer et al., 1986), which was applied only to the model layers below 10 hPa, together with the damping effect of the sponge-layer friction, which was applied to the top two model layers (Fig. 8d). Other types of parameterized forcing on the mean flow, such as surface friction and convection, are ignored because they are either confined to the planetary boundary layer or are relatively unimportant. For all plots in Fig. 8, the forcing has been converted to tendencies of the zonal wind in m/s/day.

ACPD
6, 9085–9121, 2006

EGU

Examination of Fig. 8 suggests that, in the middle atmosphere, the zonal-mean zonal wind is primarily maintained by a balance between the Coriolis force associated with the meridional transport circulation (Fig. 8b) and the parameterized forcing due to the breaking of subgrid-scale gravity waves (Fig. 8c). The contribution by the model-resolved eddy disturbances, expressed as the divergence of the EP fluxes (Fig. 8a), is secondary. For example, in the northern high latitudes near the mesopause the deceleration of the mesospheric westerly jets in January by the breaking of gravity waves reaches about 30 m/s/d, while the deceleration by the EP-flux divergence is only about 10 m/s. In the southern high latitudes near the mesopause the forcing of the zonal winds by the meridional transport circulation is almost entirely balanced by the forcing due to gravity-wave breaking, with minor contributions from the sponge-layer friction. The contribution by the model-resolved eddy disturbances is negligible.

The situation in the troposphere and middle to lower stratosphere is completely different from that in the mesosphere. The balance is achieved primarily between the forcing due to the transport circulation (Fig. 8b) and the model-resolved eddy disturbances, that is, the EP-flux divergence (Fig. 8a). Compared to the EP-flux divergence (Fig. 8a), the forcing due to the breaking of non-stationary (Fig. 8c) gravity waves is negligible. The forcing due to topographic gravity-wave breaking reached about 3 m/s/d in the northern middle latitude near the tropopause and in the lower stratosphere (Fig. 8d). The sign and magnitude are consistent with some simple model estimates (Alexander and Rosenlof, 1996; Ray et al., 1998).

The above analysis suggests that in the mesosphere and lower thermosphere strong forcing due to gravity-wave breaking is required to maintain the observed mean flow, to excite the strong meridional pole-to-pole transport circulation, and to enable the GCM to simulate the observed cold summer mesopause. This is especially true in the summer mesosphere where the forcing due to the model-resolved eddy disturbances is much weaker than in the winter mesosphere.

4.4 Equatorial winds – SAO and QBO

The semi–annual oscillation (SAO) and the quasi–biennial oscillation (QBO) are the most intriguing features of the observed tropical atmospheric circulation. We examine how they are simulated by the UIUC MST-GCM for the five cases of gravity-wave parameterization. For SAO, we present in Fig. 9 the 8-year-averaged monthly mean zonal-mean zonal winds at the equator from 100 hPa to the top of the model, together with the CIRA-86 observation. The observed equatorial zonal wind (Fig. 9a) varies with season above the middle stratosphere, and oscillates between westerly and easterly in the mesosphere. In the upper stratosphere between 10 and 1 hPa, the easterly wind reaches its first maximum in December–January and second maximum in July-August. In the middle mesosphere near 0.1 hPa, the westerly wind reaches its first maximum in March-April and second maximum in September–October. For the case of Rayleigh friction, the model simulates an SAO-like oscillation in the upper stratosphere and mesosphere, but with a strong easterly bias. The strongest easterly is displaced from the upper stratosphere in the observation (Fig. 9a) to the lower mesosphere (Fig. 9b). Also, there is no downward phase propagation. For the case of AD1999, the model simulates a strong seasonal oscillation of the zonal wind, but the downward phase propagation is too fast. For the cases of AR2003 and AR2003_M, the model is able to capture the observed SAO with a rather realistic magnitude and propagation phase speed, although the easterly winds in the upper stratosphere are still too weak.

The model failed to simulate the QBO in any of the five experiments (figures not shown). As shown in Table 1, the parameters for the cases of AR2003 and AR2003_M were prescribed differently for the tropics and extratropics based on the observational constraints derived from satellite observations and UK-METO analysis in the stratosphere. Alexander and Rosenlof (2003) presented three options (see Table 2 of their paper) for setting the parameters in the tropics, one for a best fit of the QBO at 32 hPa, one for a best fit of the SAO at 1 hPa, and the other for an overall fit in the tropics. For

the experiment AR2003, we took the option for the overall tropics fit. For the experiment AR2003_M, when tuning the parameters, we focused primarily on the extratropical temperature and circulation, especially the cold summer mesopause. The possibility of having the UIUC MST-GCM simulate the QBO with the AD parameterization is by no means exhausted here. Recently, Tan and Pawson (personnel communication) implemented the AD1999 parameterization in the NASA GEOS-4 GCM. After employing a set of parameters that are quite different from those recommended by Alexander and Rosenlof (2003), they were able to obtain a low-frequency oscillation in the tropical stratosphere that resembles the QBO. On the other hand, inferring from the studies by Takahashi and Shiobara (1995) and Takahashi (1999), probably with a much higher vertical resolution the GCM would be able to simulate the QBO, no matter what kind of parameterization for gravity-wave breaking is used. Nevertheless, the experiments with the AR2003 parameters that were constrained by observations in the tropics simulate much better the SAO. The result is encouraging and shows the obvious advantages of constraining parameters by observations compared to tuning that is at times arbitrary.

5 Conclusions

To study the impact of solar variability on atmospheric chemical composition and climate, a 40-layer GCM extending up to about 100 km has been developed at the University of Illinois at Urbana-Champaign based on the UIUC 24-layer ST-GCM (Yang et al., 2000). Efforts have been made to simulate better the temperature and circulation of the middle atmosphere because of their great impact on middle atmospheric chemical reactions and transport. In addition to the updates of the solar and longwave radiative transfer routines, attention has been paid to a better representation of the forcing of the mean flow due to gravity-wave breaking in the middle atmosphere. In this paper we have documented the sensitivity of the middle atmospheric temperature and circulation in the UIUC 40-layer MST-GCM to the treatment of subgrid-scale gravity-wave forcing. Four sensitivity experiments were performed. The forcing due to the break-

ing of non-stationary gravity waves in the middle atmosphere was represented first by Rayleigh friction, and then by the parameterization of Alexander and Dunkerton (1999) with three different sets of parameters based on the AD1999 and AR2003 papers. By making use of satellite observations and the UK Met Office-analyzed wind and temperature fields, AR2003 derived estimates of gravity-wave mean-flow forcing, and then inferred constraints on gravity waves that initiate near the tropopause and dissipate in the stratosphere. The parameters in the AD1999 paper were less constrained by observations and thus offer more freedom for tuning. In all experiments the Palmer et al. (1986) parameterization was included to treat the breaking of topographic gravity waves in the troposphere and lower stratosphere.

The simulated middle atmospheric temperature and circulation exhibit a large sensitivity to the parameterized sub-grid gravity-wave forcing. The two experiments with Rayleigh friction and the AD1999 set of parameters failed to simulate the westerly jet in the mesosphere, and produced a distorted stratospheric westerly jet that had its axis tilted towards the pole, opposite to the observed, and a jet core displaced from its observed location in the high-latitude lower stratosphere to the mid-latitude upper stratosphere. The experiment with the AR2003 set of parameters improved the simulation of the westerly jet. The location and vertical orientation of the jet core were closer to the observations, although biases still exist. The SAO was also simulated in the AR2003 and AR2003_M experiments, in which the parameters for gravity waves in the tropics were set differently from those outside the tropics. This improvement demonstrates the value of observational constraints on gravity-wave characteristics.

For the cases of Rayleigh friction and AD1999, as well as AR2003, the GCM was not able to simulate the observed reversal of the zonal winds from easterly to westerly in the summer mesosphere near the mesopause. The meridional transport circulation was very weak, hence the adiabatic cooling in the summertime upper mesosphere and lower thermosphere was insufficient. Consequently, large warm biases of up to 50°C occurred near the summer mesopause. For the case of AR2003_M, in which the forcing due to gravity-wave breaking was enhanced and reached more than 100 m/s/day near

ACPD
6, 9085–9121, 2006

EGU

the summer mesopause, the GCM produced a much stronger meridional transport circulation than for the other three cases. As a result the model was able to reduce the warm biases, and slowdown the easterly winds.

Budget analysis indicates that, for the UIUC 40-layer MST-GCM, the zonal-mean zonal wind in the middle atmosphere is primarily maintained by the balance between the Coriolis force associated with the meridional transport circulation and the parameterized gravity-wave forcing. The contribution by the model-resolved wave-mean interaction in terms of EP-flux divergence was secondary. The situation in the troposphere is totally different. The balance was achieved primarily by the forcing due to transport circulation and EP-flux divergence. In the upper troposphere and lower stratosphere, stationary (topographic) gravity waves act to slow down westerly winds, with the forcing magnitude reached about ~3.0 m/s/day in January.

In the mesosphere and lower thermosphere, strong forcing due to gravity-wave breaking is required to maintain the observed mean flow, to excite the strong meridional pole-to-pole transport circulation, and to simulate the reversed pole-to-pole temperature gradient near the mesopause. This need of strong gravity-wave forcing has been pointed out in the 1980's (e.g., Garcia and Solomon, 1985). Recently, Norton and Thuburn (1999) also found similar sensitivity of the mesospheric circulation and temperature to the strength of gravity-wave forcing in the Extended UGAMP GCM, which uses a modified version of Palmer et al. (1986) gravity-wave scheme to account for the subgrid-scale gravity-wave forcing through the atmosphere.

Even though in recent years considerable advances have been made in both the observation and theoretical understanding of middle atmospheric gravity waves (Fritts and Alexander, 2003), parameterization schemes suitable for use in middle atmospheric GCMs are still in the developing stage. Almost all current schemes (e.g., Medvedev and Klaasen, 1995; Hines, 1997a, b; Alexander and Dunkerton, 1999; Warner and McIntyre, 2001) need a set of predetermined parameters that are not all well constrained by observations; therefore, tuning is often the inevitable option. The input parameters for the AD scheme that we chose in this study are not unique, and definitely

ACPD
6, 9085–9121, 2006

EGU

are model dependent. The improvement in the simulation of stratospheric westerly jet and the SAO with the AR2003 set of parameters is encouraging and demonstrates the value of observational constraints. On the other hand, the need for extensive tuning of the parameters to simulate the observed cold summer mesopause suggests that the AR2003 parameters optimized for gravity waves dissipating in the stratosphere is, as expected, not applicable everywhere. This calls for more observations of gravity-wave activities in the upper atmosphere.

Acknowledgements. This material is based upon work supported by the National Aeronautics and Space Administration under Award No. NAG5-10942. Any opinions, findings, and conclusions or recommendations expressed in this publication are those of the authors and do not necessarily reflect the views of the National Aeronautics and Space Administration. The authors thank M. J. Alexander for providing us the code of gravity-wave forcing parameterization, and V. I. Fomichev for the code of non-LTE radiative transfer in the upper atmosphere.

References

Alexander, M. J. and Dunkerton, T. J.: A spectral parameterization of mean-flow forcing due to breaking gravity waves, J. Atmos. Sci., 56, 4167–4182, 1999.

Alexander, M. J. and Rosenlof, K. H.: Nonstationary gravity wave forcing of the stratospheric zonal mean wind, J. Geophys. Res., 101, 23 465–23 474, 1996.

Alexander, M. J. and Rosenlof, K. H.: Gravity-wave forcing in the stratosphere: Observational constraints from the Upper Atmosphere Research Satellite and implications for parameterization in global models, J. Geophys. Res., 108(D19), 4597, doi:10.1029/2003JD003373, 2003.

Andrews, D. G. and McIntyre, M. E.: Planetary waves in horizontal and vertical shear: The generalized Eliassen-Palm relation and the mean zonal acceleration, J. Atmos. Sci., 33, 2031–2048, 1976.

Andronova, N. G., Rozanov, E., Yang, F., Schlesinger, M. E., and Stenchikov, G. L.: Radiative forcing by volcanic aerosols from 1850 through 1994, J. Geophys. Res., 104, 16 807–16 826, 1999.

Beagley, S. R., Grandpre, J. D., Koshyk, J. N., McFarlane, N. A., and Shepherd, T. G.: Radiative–dynamical climatology of the first–generation Canadian middle atmosphere model, Atmosphere–Ocean, 35, 293–331, 1997.

Chou, M. D. and Suarez, M. J.: An efficient thermal infrared radiation parameterization for use in General Circulation Models. Technical Report Series on Global Modeling and Data Assimilation, National Aeronautical and Space Administration/TM–1994–104606, 3, 85 pp, 1994.

Chou, M. D. and Suarez, M. J.: A solar radiation parameterization for atmospheric studies. Technical Report Series on Global Modeling and Data Assimilation, National Aeronautical and Space Administration/TM–1999–104606, 15, 40 pp, 1999.

Fleming, E. L., Chandra, S., Schoeberl, M. R., and Barnett, J. J.: Monthly mean global climatology of temperature, wind, geopotential height, and pressure for 0–120 km. NASA Tech. Memo. NASA TM-100697, 85 pp, 1988.

Fleming, E. L., Chandra, S., Barnett, J. J., and Corney, M.: Zonal mean temperature, pressure, zonal wind, and geopotential height as functions of latitude, COSPAR International Reference Atmosphere: 1986, Part II: Middle Atmosphere Models, Adv. Space Res., 10, No. 12, 11–59, 1990.

Fomichev, V. I., Blanchet, J.-P., and Tuner, D. S.: Matrix parameterization of the 15 micro CO_2 band cooling in the middle and upper atmosphere for variable CO2 concentration, J. Geophys. Res., 103, 11 505–11 528, 1998.

Fritts, D. C. and Alexander, M. J.: Gravity wave dynamics and effects in the middle atmosphere, Rev. Geophys., 41(1), 1003, doi:10.1029/2001RG000106, 2003.

Fritts, D. C. and Lu, W.: Spectral estimates of gravity wave energy and momentum fluxes, II, Parameterization of wave forcing and variability, J. Atmos. Sci., 50, 3695–3713, 1993.

Garcia, R. R. and Solomon, S: The effect of breaking gravity waves on the dynamics and chemical composition of the mesosphere and lower thermosphere, J. Geophys. Res., 90, 3850–3868, 1985.

Gleckler, P.: AMIP Newsletter, No. 9. WNGE Atmospheric Model Intercomparison Project, Livermore, 8 pp, 1999.

Hamilton, K. (Ed.): Gravity Wave Processes and Their Parameterization in Global Climate Models, Springer-Verlag, New York, 404 pp, 1997.

Hansen, J. A., Russell, G., Rind, D., Stone, P., Lacis, A., Lebedeff, S., Ruedy, R., and Travis, L.: Efficient three–dimensional global models for climate studies: Models I and II, Mon. Wea.

Rev., 111, 609–662, 1983.
Hines, C. O.: Doppler-spread parameterization of gravity-wave momentum deposition in the middle atmosphere, 1, Basic formulation, J. Atmos. Sol. Terr. Phys., 59, 371–386, 1997a.
Hines, C. O.: Doppler-spread parameterization of gravity-wave momentum deposition in the middle atmosphere, 2, Broad and quasi monochromatic spectra, and implementation, J. Atmos. Sol. Terr. Phys., 59, 387–400, 1997b.
Holton, J. R. and Alexander, M. J.: The role of waves in the transport circulation of the middle atmosphere, in: Atmospheric Science Across the Stratopause, Geophys. Monogr. Ser., vol. 123, edited by: Siskind, D. E., Eckermann, S. D., and Summers, M. E., 21–35, AGU, Washington, D. C., 2000.
Holton, J. R. and Wehrbein, W. M.: A numerical model of the zonal mean circulation of the middle atmosphere, Pure Appl. Geophys., 118, 284–306, 1980.
Kalnay, E., Kanamitsu, M., Kistler, R., Collins, W., Deaven, D., Gandin, L., Iredell, M., Saha, S., White, G., Woollen, J., Zhu, Y., Leetmaa, A., Reynolds, R., Chelliah, M., Ebisuzaki, W., Higgins, W., Janowiak, J., Mo, K. C., Ropelewski, C., Wang, J., Jenn, R., and Joseph, D.: The NCEP/NCAR 40–year reanalysis project, Bull. Amer. Meteor. Soc., 77, 437–471, 1996.
Langematz, U. and Pawson, S.: The Berlin troposphere–stratosphere–mesosphere GCM: Climatology and forcing mechanism, Quart. J. Roy. Meteor. Soc., 123, 1075–1096, 1997.
Lindzen, R. S.: Turbulence and stress owing to gravity wave and tidal breakdown, J. Geophys. Res., 86, 9709–9714, 1981.
Lindzen, R. S. and Holton, J. R.: A theory of the quasi-biennial oscillation, J. Atmos. Sci., 25, 1095–1107, 1968.
Lott, F. and Miller, M. J.: A new subgrid-scale orographic drag parameterization: Its formulation and testing, Q. J. R. Meteorol. Soc., 123, 101–127, 1997.
Manzini E. and Bengtsson, L.: Stratospheric climate and variability from a general circulation model and observations, Clim. Dyn., 12, 615-639, 1996.
Manzini, E. and McFarlane, N. A.: The effect of varying the source spectrum of a gravity wave parameterization in a middle atmosphere general circulation model, J. Geophys. Res., 103, 31 523–31 539, 1998.
McClatchey, R. A., Fenn, R. W., Selby, J. E. A., Volz, F. E., and Garing, J. S.: Optical Properties of the Atmosphere, Air Force Cambridge Research Laboratories, AFCRL–72–0497, 221 pp, 1972.
McFarlane, N. A.: The effect of orographically excited gravity wave drag on the general circula-

tion of the lower stratosphere and troposphere, J. Atmos. Sci., 44, 1775–1800, 1987.
Medvedev, A. S. and Klaassen, G. P.: Vertical evolution of gravity wave spectra and the parameterization of associated wave drag, J. Geophys. Res., 100, 25 841–25 853, 1995.
Medvedev, A. S., Klaassen, G. P. and Beagley, S. R.: On the role of an anisotropic gravity wave spectrum in maintaining the circulation of the middle atmosphere. Geophys. Res. Lett., 25, 509–512, 1998.
Norton, W. A. and Thuburn, J.: Sensitivity of mesospheric mean flow, planetary waves, and tides to strength of gravity wave drag, J. Geophys. Res., 104 , 30 897–30 912, 1999.
Palmer, T. N., Shutts, G. J., and Swinbank, R.: Alleviation of a systematic westerly bias in general circulation and numerical weather prediction models through an orographic gravity wave drag parameterization, Quart. J. Roy. Meteor. Soc., 112, 1001–1039, 1986.
Peixóto, J. P. and Oort, A. H.: Physics of Climate, American Physical Society (New York), 520 pp, 1992.
Randel, W. and coauthors: The SPARC intercomparison of middle-atmosphere climatology. J. Climate, 17, 986-1003, 2004.
Ray, E. A., Alexander, M. J., and Holton, J. R.: An analysis of the structure and forcing of the equatorial semiannual oscillation in zonal wind, J. Geophys. Res., 103, 1759–1774, 1998.
Rozanov, E., Zubov, V., Schlesinger, M. E., Yang, F. and Andronova, N.: Three-dimensional simulations of ozone in the stratosphere and comparison with UARS data, Phys. Chemi. Earth, 24, 459–463, 1999a.
Rozanov, E., Zubov, V., Schlesinger, M. E., Yang, F., and Andronova, N: The UIUC 3–D Stratospheric Chemical Transport Model: description and evaluation of the simulated source gases and ozone, J. Geophys. Res., 104, 11 755–11 781, 1999b.
Rozanov, E., Schlesinger, M. E., Andronova, N. G., Yang, F., Malyshev, S. L., Zubov, V. A., Egorova, T. A., and Li, B.: Climate/chemistry effects of the Pinatubo volcanic eruption simulated by the UIUC stratosphere/troposphere GCM with interactive photochemistry, J. Geophys. Res., 107(D21), 4594, doi:10.1029/2001JD000974, 2002.
Rozanov, E., Schlesinger, M. E., Egorova, T. A., Li, B., Andronova, N. G., and Zubov, V. A.: Atmospheric response to the observed increase of solar UV radiation from solar minimum to solar maximum simulated by the University of Illinois at Urbana-Champaign climate-chemistry model, J. Geophys. Res., 109, D01110, doi:10.1029/2003JD003796, 2004.
Rozanov, E., Callis, L., Schlesinger, M., Yang, F., Andronova, N., and Zubov, V.: Atmospheric response to NOy source due to energetic electron precipitation, Geophys. Res. Lett., 32,

L14811, doi:10.1029/2005GL023041, 2005.
Shepherd, T. G., Semeniuk, K., and Koshyk, J. N.: Sponge layer feedbacks in middle-atmosphere models, J. Geophys. Res., 101(D18), 23 447–23 464, 1996.
Strobel, D. F.: Parameterization of the atmospheric heating rate from 15 to 120 km due to O2 and O3 absorption of solar radiation, J. Geophys. Res., 83, 6225–6230, 1978.
Swinbank, R., Lahoz, W. A., O'Neill, A., Douglas, C. S., Heaps, A. and Podd, D.: Middle atmosphere variability in the UK Meteorological Office Unified Model, Quart. J. Roy. Meteorol. Soc., 124, 1485–1526, 1998.
Swinbank, R. R. and Ortland, D. A.: Compilation of wind data for the Upper Atmosphere Research Satellite (URAS) Reference Atmosphere Project, J. Geophys. Res., 108, 4615, doi:10.1029/2002JD003135, 2003.
Takahashi, M.: Simulation of the quasi–biennial oscillation in a general circulation model, Geophys. Res. Lett., 26, 1307–1310, 1999.
Takahashi, M. and Shiobara, M.: A note on a QBO–like oscillation in the 1/5 sector CCSR/NIES GCM, J. Meteor. Soc. Japan, 73, 131–137, 1995.
Warner, C. D. and McIntyre, M. E.: An ultra-simple spectral parameterization for non-orographic gravity waves, J. Atmos. Sci., 58, 1837–1857, 2001.
Yang, F.: Radiative forcing and climatic impact of the Mount Pinatubo volcanic eruption, Ph.D. Dissertation, University of Illinois at Urbana-Champaign, pp 219, 2000.
Yang, F. and Schlesinger, M. E.: On the surface and atmospheric temperature changes following the 1991 Pinatubo volcanic eruption: A GCM study, J. Geophys. Res., 107(D8), 4073, doi:10.1029/2001JD000373, 2002.
Yang, F., Schlesinger, M. E., and Rozanov, E.: Description and performance of the UIUC 24-layer stratosphere/troposphere general circulation model, J. Geophys. Res., 105(D14), 17 925–17 954, 2000.

Table 1. Parameters of the AD scheme chosen for the four GCM experiments. Where (1) KS, the model layer and corresponding altitude (see Fig. 1) of the input/source gravity-wave momentum fluxes; (2) F_{s0}, a constraint on the integrated momentum fluxes, which in turn controls an intermittency factor defined in the AD scheme; (2) c_0 and $\widehat{c}$, the ground-based phase speed and intrinsic phase speed; (4) B_m, the peak momentum flux per unit mass for the broad non-stationary source spectrum of gravity waves; (5) Flag defines at what phase speed the input momentum flux peaks. For Flag=0, B_m peaks at c_0=0; For Flag=1, B_m peaks at $\widehat{c}$=0; (6) c_w, the half-width of the broad spectrum in phase speed; (7) L, horizontal wavelength of gravity waves; (8) Δc and n_c, the spectral resolution and number of spectral points; (9) U_0, zonal wind at the source layer KS; U, zonal wind in the middle mesosphere; (10) NH and SH represent the Northern and Southern Hemisphere, respectively. The notations for parameters (2) to (8) follow AD1999 and AR2003 and were described in detail therein.

AD Parameters	AD1999	AR2003		AR2003_M	
		Tropics (15° S–15° N)	Outside Tropics	Tropics (15° S–15° N)	Outside Tropics
KS	10	16	16	16	16
F_{s0} (Pascal)	0.006	If U_0<0, –0.0005 If U_0>0, 0.0004	NH: 0.0014 SH: 0.0015	If U_0<0, –0.001 If U_0>0, 0.0008	NH: 0.0021 SH: 0.00225
B_m (m^2/s^2)	0.4	If U_0<0, 10 If U_0>0, 1	1.0	If U_0<0, 10 If U_0>0, 1	0.5
Flag	0	1	0	1	0
c_w (m/s)	40	If U_0<0, 25 If U_0>0, 80	If U<0, 40 If U>0, 5	If U_0<0, 25 If U_0>0, 80	20
L (km)	300	4000	100	2000	100
Δc (m/s)	1.0	1.0	1.0	1.0	1.0
n_c	121	121	121	121	121

ACPD
6, 9085–9121, 2006

EGU

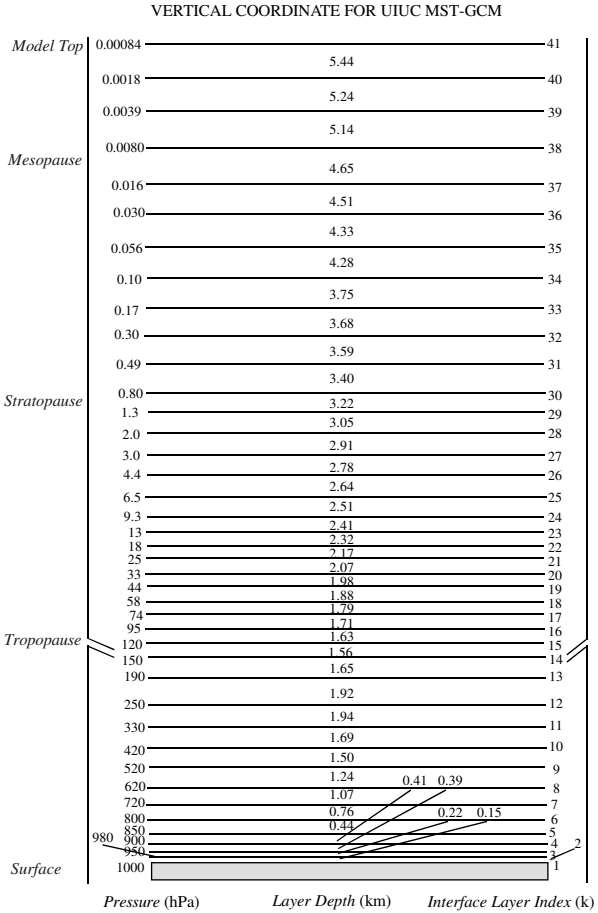

Fig. 1. Vertical structure of the UIUC 40-layer MST-GCM.

ACPD
6, 9085–9121, 2006

GCM temperature and circulation sensitivity to GWD forcing

F. Yang et al.

EGU

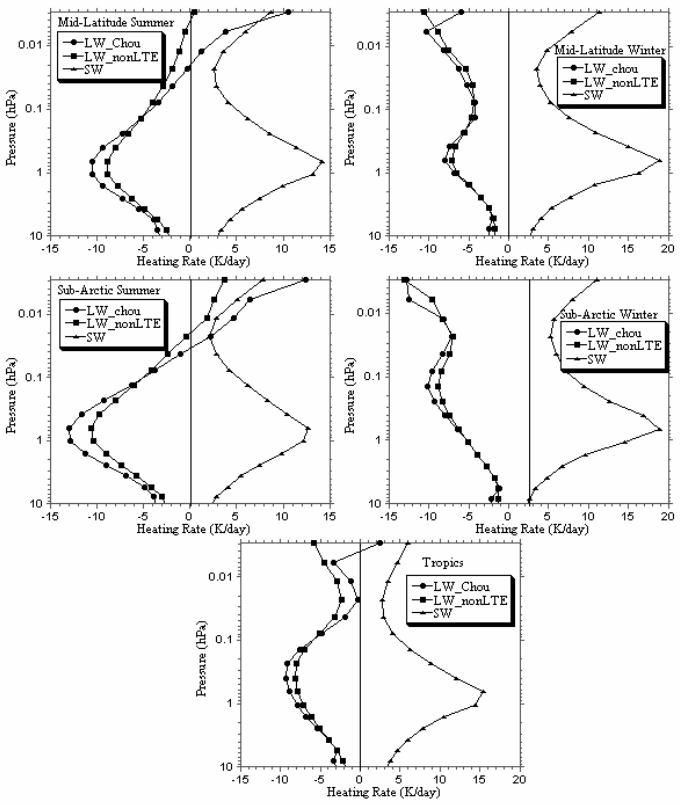

Fig. 2. Long-wave heating rates computed by the Chou-Suarez (as LW_Chou) and Fomichev et al. (1998) (as LW_nonLTE) schemes, respectively, for five standard atmospheric profiles. The Fomichev scheme computes LW heating in both LTE and non-LTE conditions, while the Chou-Suarez scheme is not applicable for non-LTE condition and is only suitable for the atmosphere below mesopause. Solar heating (SW) was also included for reference (see text for details).

ACPD
6, 9085–9121, 2006

EGU

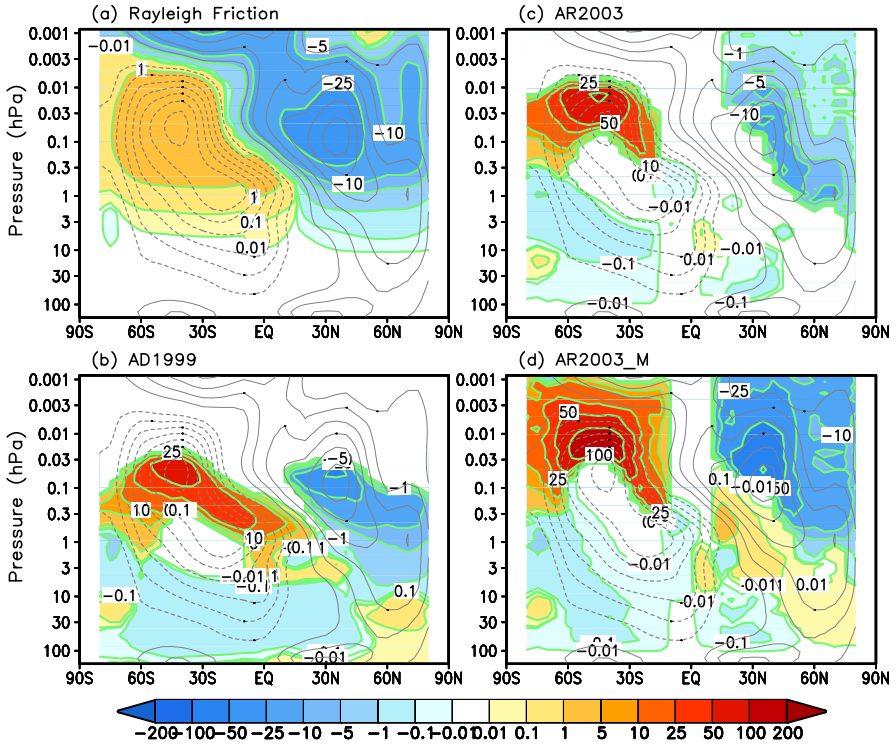

Fig. 3. Mean-flow forcing (color shadings edged by thick green lines) of zonal-mean zonal winds (m/s/day) due to breaking of gravity waves in January. For reference, the background zonal-mean zonal winds are plotted as black contours with a 10 m/s interval. Dotted lines are for easterly winds, and unbroken lines for westerly winds. The zero contour line is omitted.

ACPD
6, 9085–9121, 2006

EGU

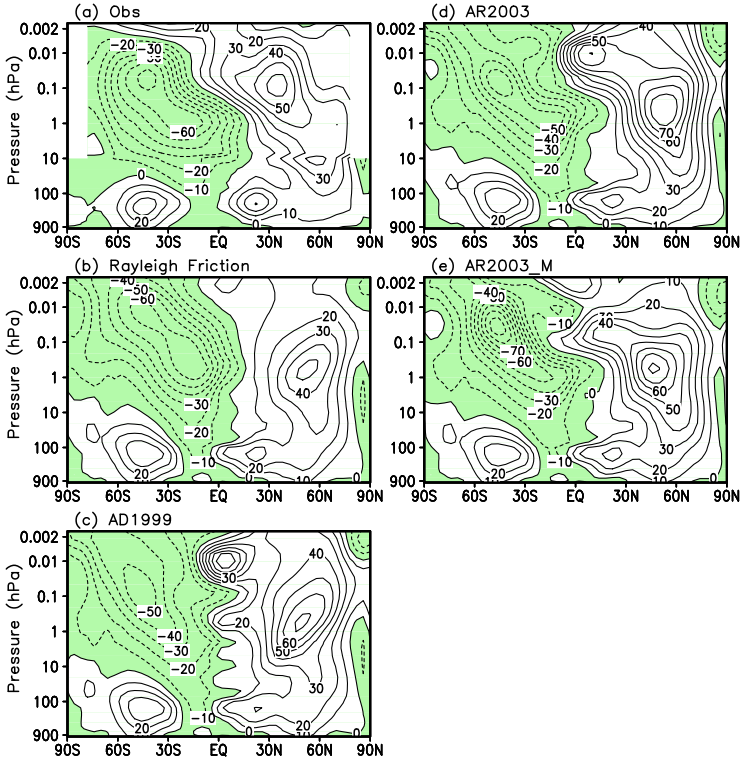

Fig. 4. Zonal-mean zonal wind in January for observations and for simulations by the UIUC 40-layer MST-GCM. The observations consist of NCEP/NCAR Reanalysis averaged for the 1979–1995 period below 10 hPa and CIRA-86 data above. All simulation results are 8-year averages. The contour interval is 10 m/s. Easterly winds are shaded.

ACPD
6, 9085–9121, 2006

EGU

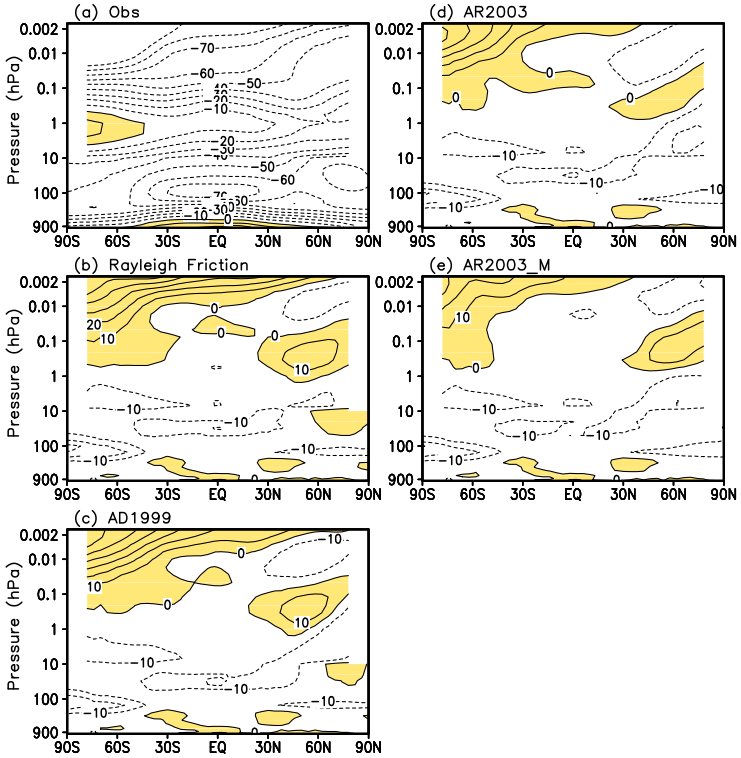

Fig. 5. Zonal-mean temperatures in January for observations and the differences from observations simulated by the UIUC 40-layer MST-GCM. The observations consist of NCEP/NCAR Reanalysis averaged for the 1979–1995 period below 10 hPa and CIRA-86 data above. All simulation results are 8-year averages. The contour interval is 10°C. Shadings indicate warm biases for simulations and above-zero temperature for the observation.

ACPD
6, 9085–9121, 2006

EGU

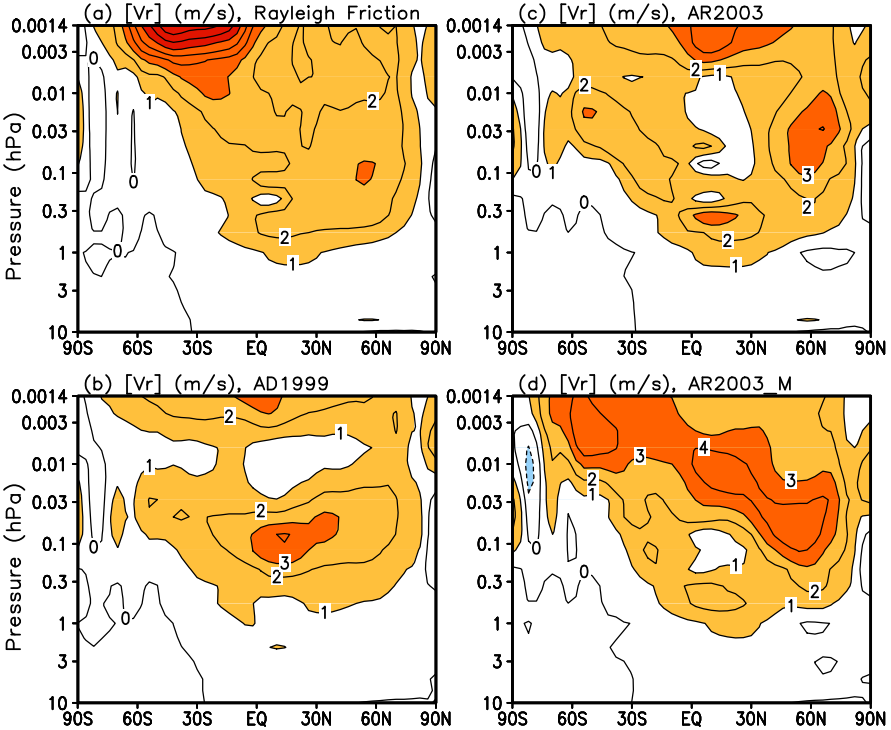

Fig. 6. Residual meridional wind between 10 hPa and the model's top in January. The contour interval is 1.0 m/s. Positive values indicate northward motion.

ACPD
6, 9085–9121, 2006

EGU

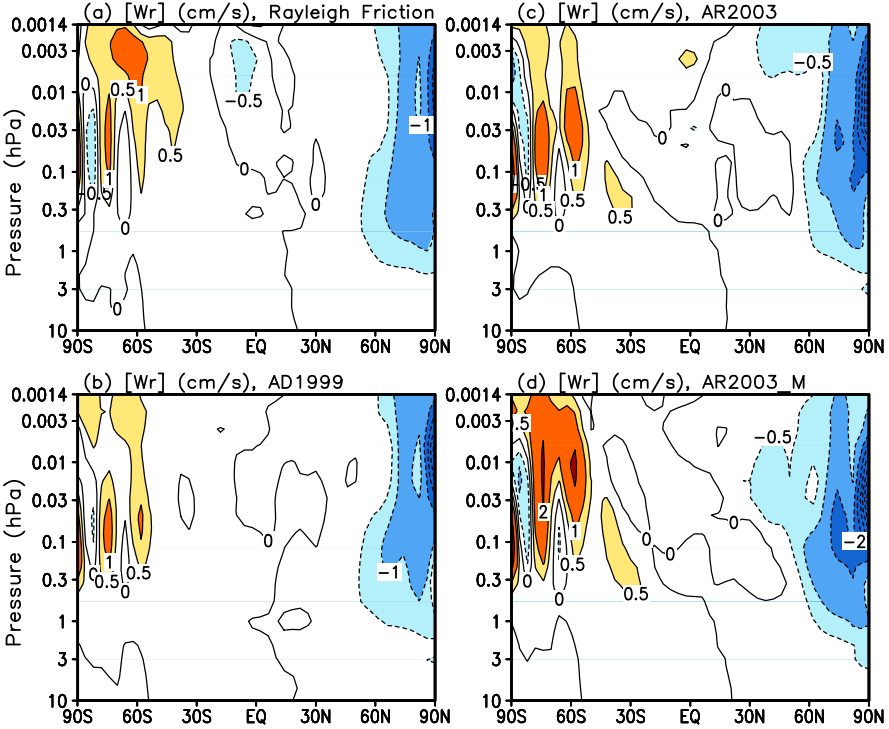

Fig. 7. Residual vertical wind between 10 hPa and the model's top in January. The contour interval is 1.0 cm/s with ±0.5 cm/s lines added. Positive values indicate upward motion.

ACPD
6, 9085–9121, 2006

EGU

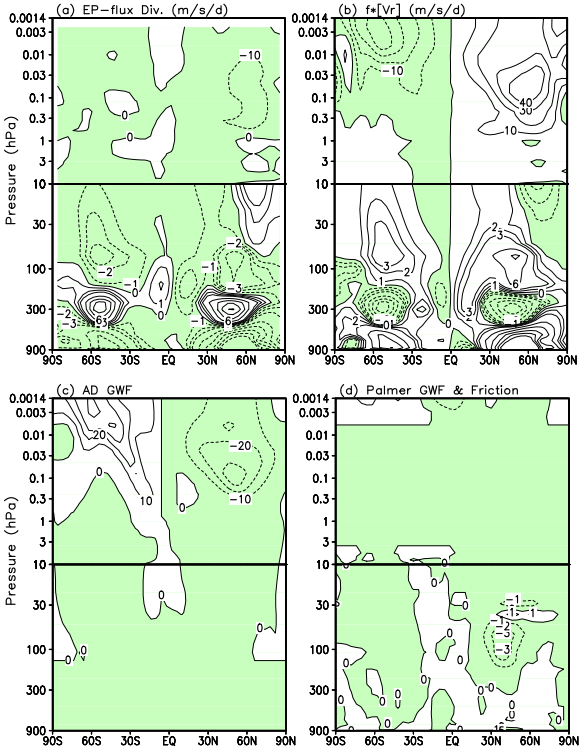

Fig. 8. Accelerations of the zonal-mean zonal wind in January for the case of AR2003_M due to **(a)** EP-flux divergence, **(b)** residual meridional wind, **(c)** the breaking of non-stationary gravity waves from the AD parameterization, and **(d)** the breaking of topographic gravity waves from the Palmer et al. (1986) parameterization, which was applied only below 10 hPa, and the "sponge-layer" friction, which was applied to the top two layers of the model. Above 10 hPa, the contour interval is 10 m/s/day. Below 10 hPa, the contour interval is 3 m/s/day in (a) and (b), with the ±1 and ±2 contours added, and 1 m/s/day in (c) and (d). Negative values indicate westward wind acceleration (slowdown of westerly winds).

ACPD
6, 9085–9121, 2006

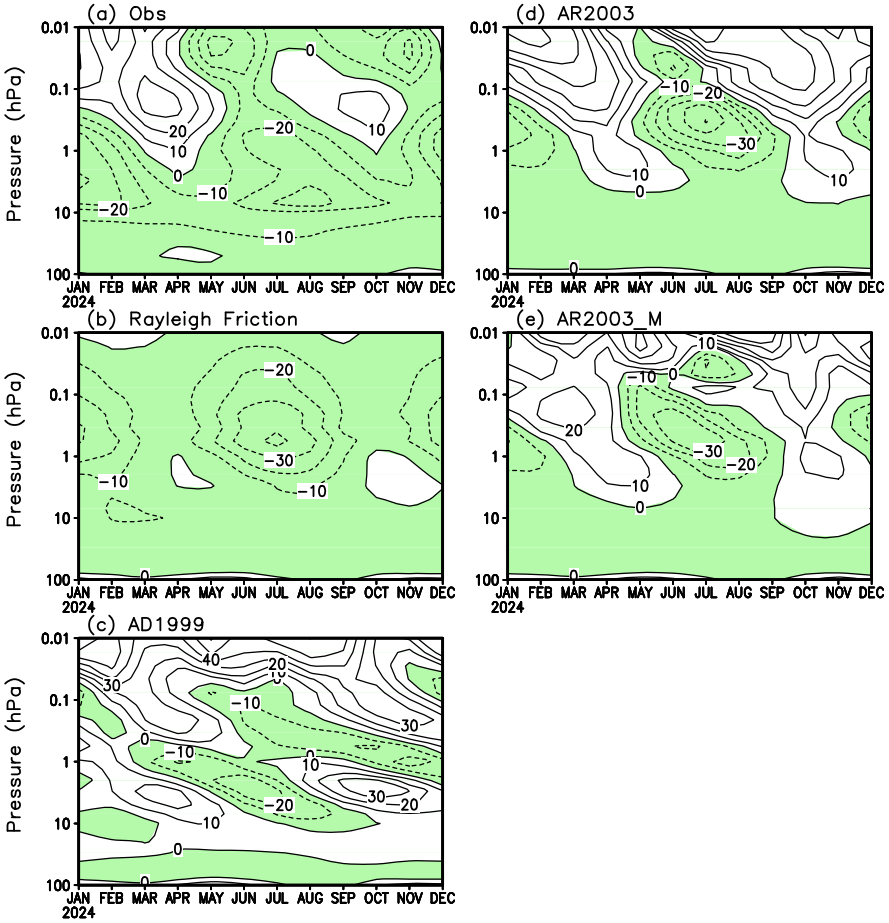

Fig. 9. Monthly zonal-mean zonal winds at the equator in the upper atmosphere. The observation above 10 hPa is CIRA-86. All simulations are 8-year averages. The contour interval is 10 m/s. Easterly winds are shaded.

ACPD
6, 9085–9121, 2006